VENTRICULAR HYPERTROPHY: ADVANTAGES AND CONSEQUENCES

ANNE L. TAYLOR, M.D.

THURSDAY, SEPTEMBER 21, 1989

MEDICAL GRAND ROUNDS
SOUTHWESTERN MEDICAL SCHOOL
UNIVERSITY OF TEXAS SOUTHWESTERN MEDICAL CENTER
DALLAS, TEXAS

Ventricular Hypertrophy: Advantages and Consequences

Myocardial hypertrophy is the adaptive response to sustained increases in ventricular workload. The workload stimulus provoking hypertrophy may be either a chronic increase in ventricular volume (aortic or mitral regurgitation, arteriovenous fistulae) or ventricular afterload (systemic hypertension, aortic stenosis). Hypertrophy may also be provoked by humoral substances such as catecholamines, the renin-angiotensin system (Grossman et al., 1983), thyroid hormone and copper, iron and thiamine deficiency (Maron and Ferrans, 1978). Myocardial ischemia (Bloor, 1978) results in hypertrophy of the nonaffected myocardium, and finally, hypertrophy may be genetically determined, as is the case in idiopathic hypertrophic cardiomyopathy. The element in common among all of these forms of hypertrophy is an increase in the mass of the affected ventricles which is accomplished by increase in myocyte size rather than number of myocytes, and the functional progression from adaptive advantage to eventual failure. In addition to an increase in myocyte size, there are increases in other elements of myocardium including fibrous tissue and vasculature. Proliferation of these elements may vary strikingly depending upon the stimulus to hypertrophy. For example, when hypertrophy results from excess thyroid hormone, there is evidence that new vascular elements are formed thus maintaining a normal relationship between volume of myocytes and volume of capillaries and that collagen synthesis is not increased. In contrast, when hypertrophy results from pressure overload, there is limited vascular proliferation and capillary density decreases relative to myocardium (Marcus et al., 1983b; Tomanek et al., 1986) while collagen remodeling is extensive. Myosin isoenzymes in hypertrophied myocardium may also vary dependent upon the stimulus to hypertrophy. Pressure-overload in the rat is accompanied by a shift to isoenzyme V_3, a slower activity form of the enzyme (Mercadier et al., 1981). Thus, ventricular hypertrophy is a process of considerable tissue cellular and biochemical heterogeneity rather than a simple quantitative process - there are substantial qualitative changes associated with myocardial hypertrophy. While, in general, myocardial hypertrophy has the adaptive advantage of maintaining normal cardiac output in the face of a sustained increase in workload, this is accomplished at considerable biologic expense. The disadvantageous consequences of myocardial hypertrophy are extensive and interact in a negative synergistic fashion with other common forms of heart disease.

Of the many forms of hypertrophy, the most frequently encountered in the clinical setting is that resulting from increases in afterload such as systemic hypertension or aortic stenosis. The remainder of this discussion will be confined to a discussion of the structural, functional, electrophysiologic, and coronary vascular alterations associated with compensated pressure-overload hypertrophy, thus, stressing a third important concept - in the setting of the functionally compensated hypertrophied ventricle, (hypertrophy prior to the onset of failure) biologic advantage and deleterious consequences are temporally coexistent.

Anatomic Changes.

Left ventricular hypertrophy is defined as a left ventricular mass in excess of 500 g (normal <350). In response to pressure overload, prompt acceleration of protein synthesis and inhibition of protein degradation occur (Gordon et al., 1987; Morgan et al., 1986) resulting in a net increase in myocardial mass.

Figure 1.

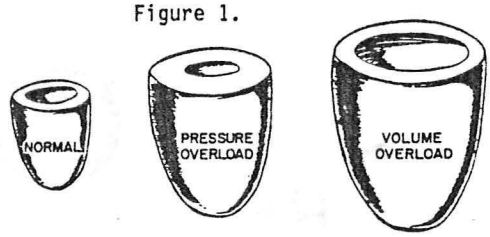

LV PRESSURE (mmHg)	117±7/10±1	226±6*/23±3*	138±7/23±2*
LVMI (gm/m^2)	71±8	206±17*	196±17*
LV WALL THICKNESS (mm)	8.2±.6	15.2±.9*	10.6±.5*
h/R	.34±.03	.56±.05*	.33±.02
σ_m (10^3 dynes/cm^2)			
PEAK SYSTOLIC	151±4	161±24	175±7
END DIASTOLIC	17±2	23±3	41±3*

*p<.01

Figure 1. Left ventricular (LV) pressure, left ventricular mass index (LVMI), wall thickness, ratio of wall thickness to radius (h/R) at end diastole, and meridional left ventricular wall stress (σ_m) in patients with normal hearts compared to those with chronic left ventricular pressure overload or volume overload. Only patients with chronic left ventricular pressure or volume overload who were well compensated and had no depression of systolic function (LV ejection fraction) were included. (Grossman et al., 1983).

The particular geometric remodeling of the ventricle is a very sensitive indicator of the nature of the stimulus to hypertrophy. Wall thickness is accomplished at the expense of cavity area in pressure overload hypertrophy. Thus the ratio of wall thickness to cavity radius (h/R) is increased (Grossman, 1983) in pressure overload hypertrophy but preserved in volume overload. Trabeculae carneae and papillary muscles also enlarge (Gould, 1968). Lengthening of the left ventricular chamber is prominent, so that the papillary muscles appear to arise nearer the MV orifice and the MV orifice, is tilted in a plane such that it is nearly parallel to the AV ring (Bloor, 1978).

Hutchins et al. (1978) have suggested that the shape of the heart develops to meet the needs of efficient filling (diastole) as well as

efficient tension development and ejection (systole). The prolate ellipse shape of the left ventricle is a compromise shape between the thin-walled sphere (most efficient geometry for diastolic filling) and a simple tubular structure (most efficient geometry for systolic pressure development). The heart hypertrophying in response to pressure overload both elongates and develops thicker walls thereby becoming more tubular.

Figure 2.

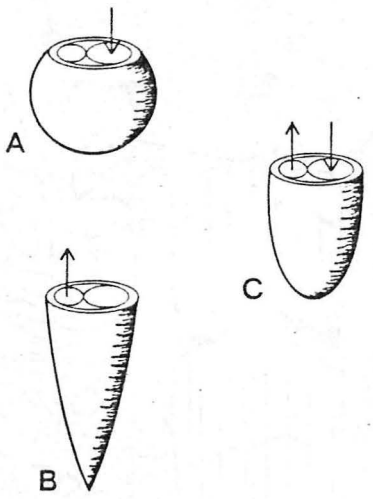

Figure 2. Diagram of possible ventricular shapes, all with the same inlet-outlet port. A, a spherical ventricle would require the least expenditure of energy for diastolic filling. B, a nearly conical ventricle would be more efficient for systole because the curvature of muscle cells is increased allowing a greater transfer of the energy of contraction to increasing intracavitary pressure. C, the prolate hemispheroid is the shape that would minimize the sum of energy expenditures in diastole and systole and is also the shape that most closely resembles the normal human left ventricle. (Hutchins et al., 1978).

Normal systolic wall stress (force per unit cross-sectional area of myocardium), (Grossman et al., 1975) and contractile efficiency are maintained; however, diastolic filling efficiency is compromised.

Changes in cellular architecture accompanying pressure overload hypertrophy are summarized below, next to the corresponding elements of normal tissue.

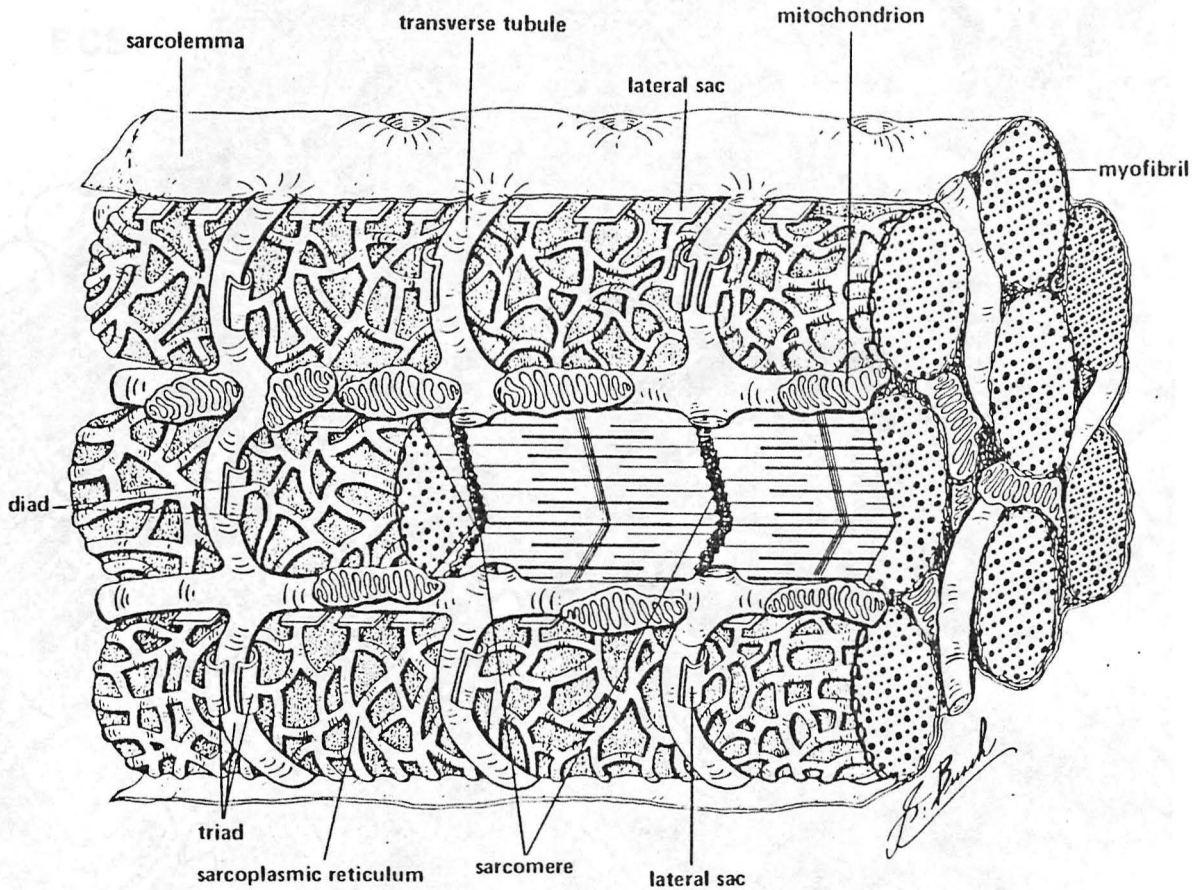

Figure 3.

Figure 3. Ordinary Working Ventricular Cell: Detail. (Legato, 1973).

Figure 4.

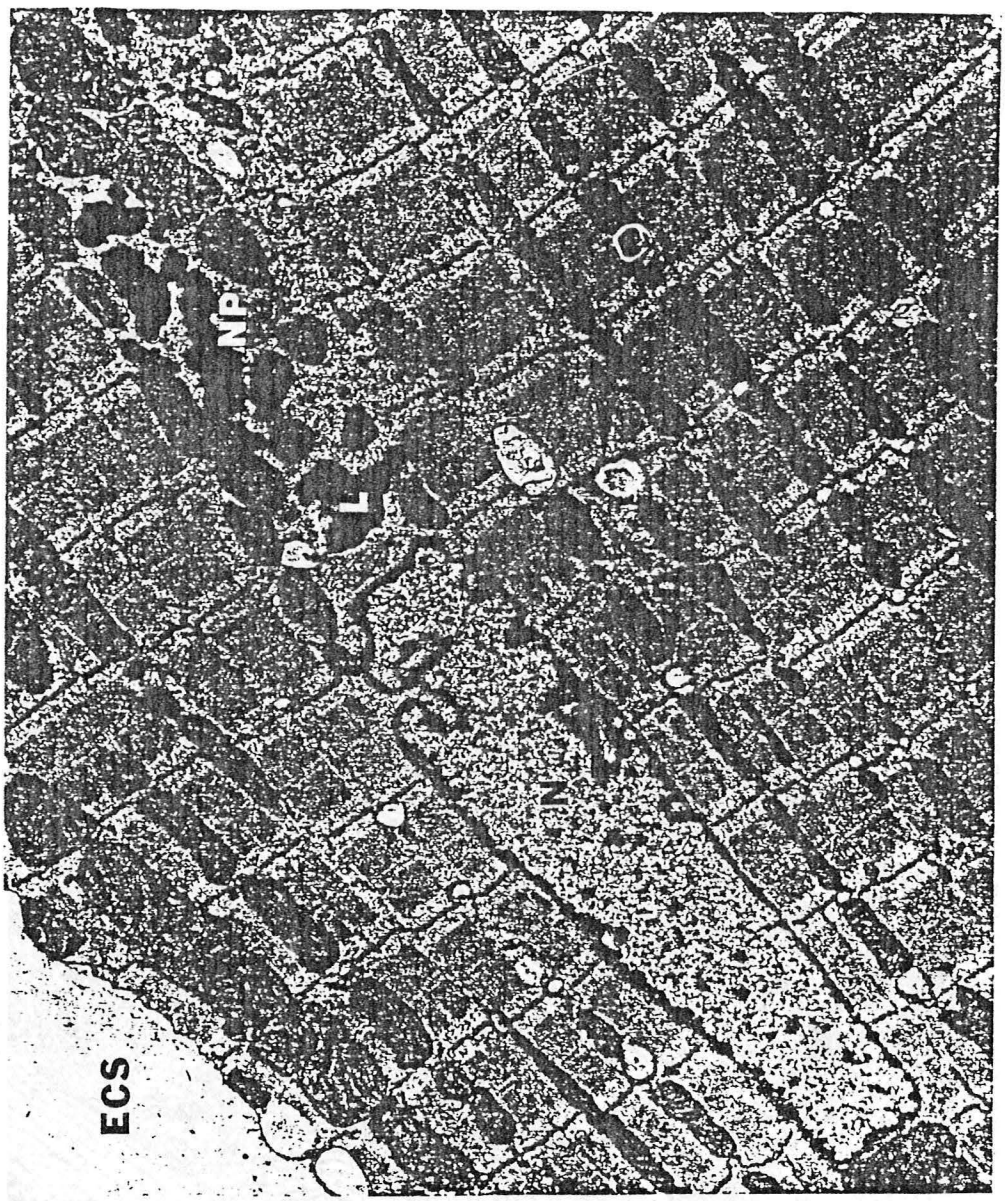

Figure 4. (Legato, 1973)

Figure 5.

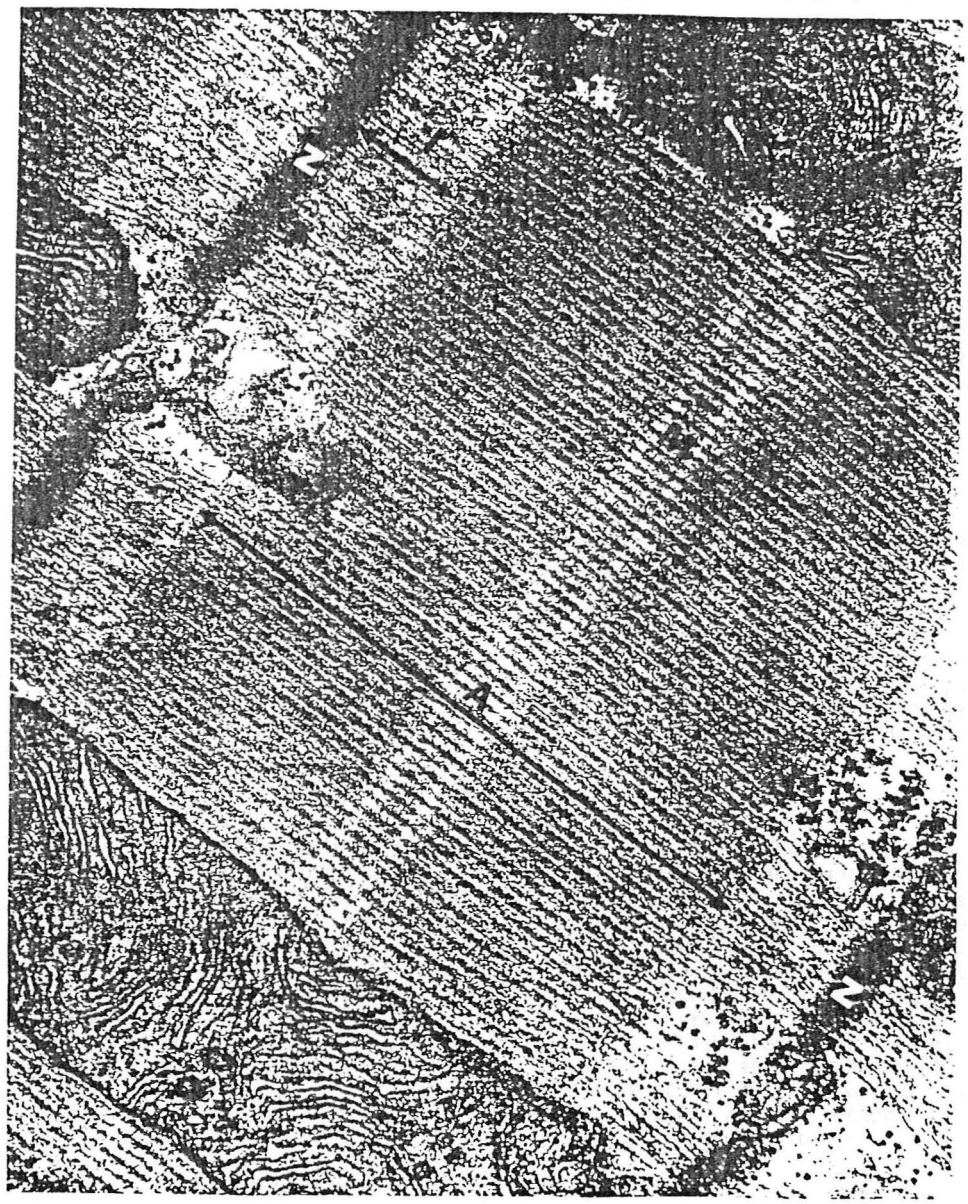

Figure 5. (Legato, 1973).

Basic Unit

Normal Myocardium	Hypertrophied Myocardium
Myofiber	
Individual myocardial cell 10-20 u diameter, 50-100 u length-myocytes are branching striated cells connected to to other myofibers by intercalated discs. Interercalated discs join cells together and provide a specialized area for facilitation transmission of action potentials.	Increased size particularly in the transverse diameter (20-60 u) rather than longitudinal dimension with considerable cell to cell size variability. Tortuosity and multiplicity of intercalated discs which are thought to be preferential sites of new sarcomere formation during cell enlargement. Overall during compensated hypertrophy, the orientation of individual myofibers remain relatively normal.

Subunits

Myofibrils	
Contractile unit composed of sarcomeres arranged in series and in parallel.	Early in pressure overload hypertrophy, increases in myofibril size occurs by increasing the numbers of sarcomeres in parallel. However, as cellular enlargement progresses increases in myofibril number occur. Over time, the organizational pattern of sarcomeres making up myofibrils may become less ordered.
Sarcomere	
Basic contractile unit consists of interdigitating thick (myosin) and thin (actin) fibers. The boundary of each sarcomere is the Z band which is the site of insertion of the thin (actin) filaments. Thin fibers are also the sites of proteins which regulate contraction such as troponin and tropomyosin.	Increase in number of sarcomeres with some disarrangement of sarcomeric units. Sarcomeres in pressure overload hypertrophy are added in parallel rather than in series as is the case with volume overload. Aggregated Z band material is often present in hypertrophied cells. This material is thought to be the site of attachment of new sarcomeres. But, excess Z band material may also be the product of disruption of myofibrils.

MYOFILAMENTS

Bundles of contractile protein filaments consisting of myosin (thick filament - forming the A band of the sarcomere) and actin (thin filament forming the I band of the sarcomere attached to the Z band). Cyclic Ca^{++} dependent crossbridging of these protein filaments produce muscle shortening. Troponin and tropomyosin, protein regulators of cyclic actin-myosin cross-bridging are located on the myofibrils.

Early in hypertrophy, all myofilaments increase in number. Late with cellular degeneration resulting from long standing hypertrophy, there is selective loss of thick (myosin) fibers with aggregations of thin fiber material.

MITOCHONDRIA

Site of ATP generation - in normal myocardium occupy about 20-30% of the cell volume. Generally closely opposed to myofibrils and sarcolemma.

Large, early (within 20 hours of imposition of pressure load) increase in mitochondrial volume fraction relative to myofibril volume fraction with return to normal ratio during stable hypertrophy. However, late in hypertrophy, the volume ratio of mitochondria to myofibrils decreases. Size heterogeneity is typically present.

SARCOLEMMA

The cell membrane controls the ionic composition of the cell and maintains electrochemical gradients. Contains ion channels for action potential generation as well as receptors for neurotransmitters and hormones.

Increases with hypertrophy, however membrane electrical capacitance is decreased suggesting that newly formed membrane may not be functionally normal.

T-TUBULES

Transmission of ion current-generated action potential from the sarcolemma to cell interior where Ca^{++} necessary for contraction is released.

Increased in area proportional to the increase in cell volume. The relative proportion of sarcolemma to T-tubule system is decreased.

Sarcoplasmic reticulum

Site of cyclic Ca^{++} uptake and release necessary for coupling of electrical excitation to mechanical contraction and relaxation.

Increases proportionately to the cell volume increase so that normal ratio is preserved.

Non Muscle Components

Collagen

Provides structural support, as well maintenance of cellular alignment. Fine collagen fibrils are generally found in and around myofibers.

Collagen content and distribution increases slowly relative to other cell components. In compensated hypertrophy of 4-88 weeks duration, collagen is increased by 4 weeks, then remained stable for up to 88 weeks. At 4 weeks, heavy collagen fibers replaced thin fibers. By 35-88 weeks, fine fibrils reappeared but dense collagenous septae were also present. At this stage cardiac output was preserved, and no necrotic changes in myocytes had appeared. Of interest both systolic and diastolic function were normal. Collagen remodeling is a slow process which then stabilizes for long periods of time.

Figure 6.

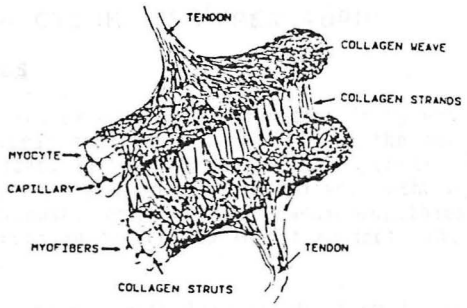

Figure 6. Schematic representation of the collagen matrix of the primate left ventricle. Groups of myocytes formed by collagen weave, are termed myofibers. Myofibers are connected to one another by strands of collagen, whereas myocyte-to-myocyte connections and myocyte and their adjacent capillaries are joined by struts of collagen. (Weber et al., 1987).

VASCULATURE

Capillary density in normal myocardium is 2 to 5 x 10^5 capillary per mm^2 myocardium. Normal capillary to myofiber ratio is 1:1.

Capillary volume does not increase with the increase in myocardial mass. Capillary lumen (but not length) selectively increases. Intercapillary distance increases.

The end stage of hypertrophy with degeneration consists of:

1. Loss of contractile elements, preferentially thick filaments (myosin).
2. Loss of specialized areas of intercellular contacts.
3. Interstitial fibrosis.
4. Preservation of other cell organelles (nuclei, mitochondria) despite loss of contractile elements.

Specific disease entities have been more frequently associated with hypertrophy with or without associated degeneration. Thus, it has been found that combined aortic stenosis and regurgitation was more likely to be associated with degenerative changes than pure aortic stenosis in which hypertrophy without degeneration was more likely. However, the authors point out that the timing and reason for surgery in these two groups are different; thus, it may not be possible to conclude that the type of hemodynamic burden determines whether or not degeneration occurs (Anversa et al., 1978; Anversa et al., 1976; Anversa et al., 1986; Bishop, 1983; Bloor, 1978; Braunwald et al., 1988; Ferrans, 1983; Goldstein et al., 1974; Gould, 1968; Jones and Ferrans, 1980; Legato, 1973; Marcus, 1983; Maron and Ferrans, 1978; Pearlman et al., 1981; Rakusan et al., 1980; Schaper et al., 1974; Weber et al., 1987; Weber et al., 1988).

MECHANICAL FUNCTION IN HYPERTROPHY

CLINICAL FINDINGS

Clinical studies of contractile function in hypertrophied myocardium are complicated by several important variables: 1) the duration and severity of the increased workload, 2) the adequacy of the hypertrophy response, 3) age of subjects, 4) the presence of other concomitant pathologic processes such as coronary artery disease, or unrelated cardiomyopathies, 5) the effects of sympathetic influences in the reflex intact subject, and finally 6) peripheral adaptive changes.

Overall, in patients with hypertrophy from hypertension (Takahashi et al., 1980) or aortic stenosis (Huber et al., 1981; Spann et al., 1980; Levine et al., 1970; Simon et al., 1970) there is a spectrum of function ranging from supernormal to congestive heart failure. In the absence of congestive failure however most indices of ventricular function are normal in adults or even above normal in children (Assey et al., 1987). One key element in the preservation of normal function appears to be the preservation of normal wall

stress. Wall stress is the force per unit cross-sectional area of myocardium (dynes/cm² myocardium).

Figure 7.

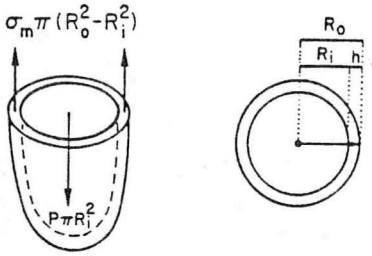

Figure 7. Diagrammatic representation of an idealized LV chamber in coronal section, looking from the front (left) and above (right). Wall thickness (h), inner radius (R_i), and outer radius (R_o) are required to calculate meridional wall stress (σ_m). This is accomplished by equating the meridional wall forces ($\sigma_m \times \pi[R_o^2 - R_i^2]$) to the pressure loading ($P\pi R_i^2$), since these must be exactly equal if the ventricle is to hold together. The same calculation applies for either an ellipsoidal or a spherical model (Grossman et al., 1975).

$$\sigma_m\pi(R_o^2-R_i^2)=P\pi R_i^2$$

$$\sigma_m = PR_i/2h(1+h/2R_i)$$

Wall stress, whether circumferential, meridional or radial, is directly related to ventricular pressure and indirectly related to wall thickness. Thus, if pressure increases, wall thickness must increase to maintain normal wall stress (Grossman et al., 1975).

Figure 8.

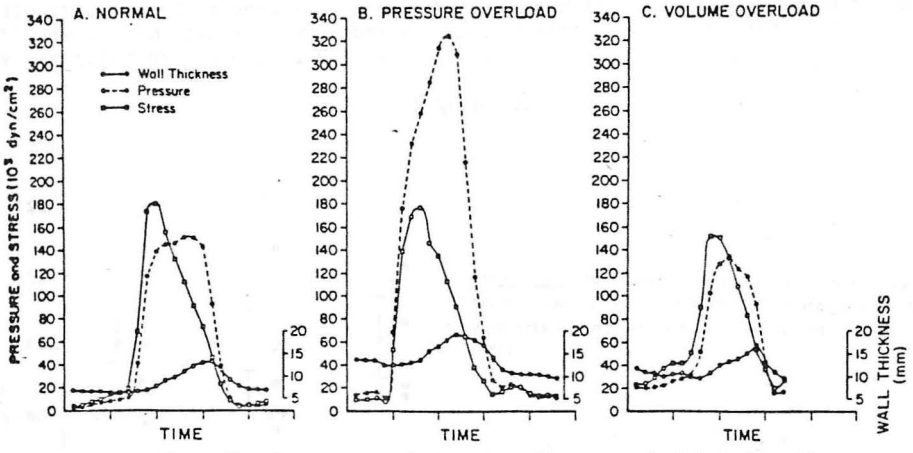

Figure 8. A comparison of changes in LV pressure (solid dots), wall thickness (open dots), and meridional stress (open squares) throughout the cardiac cycle for representative normal, pressure-overloaded, and volume-overloaded left ventricles. Measurements are plotted here at 40-ms intervals. In the pressure-overloaded ventricle (B), the markedly elevated systolic pressure is exactly counterbalanced by increased wall thickness with the result that wall stress remains normal. In the volume-overloaded ventricle (C), peak systolic stress is normal but end diastolic stress is significantly increased. (Grossman et al., 1975).

Ejection fraction (the percentage of blood ejected by the ventricle during systole) may then be closely coupled to wall stress. Linear regression shows the decreasing ejection fraction as wall stress increases.

Figure 9.

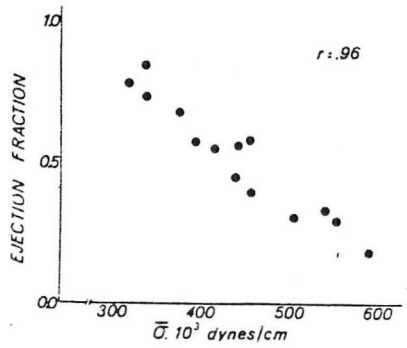

Figure 9. Relationship between the left ventricular ejection fraction and mean systolic midwall circumferential stress (σ) in patients with pure aortic stenosis and varying degrees of systolic dysfunction. A close, inverse correlation is observed. (Grossman et al., 1983).

The age at which pressure overload is applied may influence the amount of increase in wall thickness and thus, wall stress and ejection fraction. Assey et al. compared left ventricular mass, ejection fraction and wall stress in three groups of patients with similar transaortic pressure gradients. The groups were as follows: young children (<10 years) with aortic stenosis, older children and young adults with congenital aortic stenosis and adults with acquired aortic stenosis. Age matched controls for each group were also studied. No patients or controls had abnormal ejection fraction. Left ventricular pressure gradients were similar.

Figure 10.

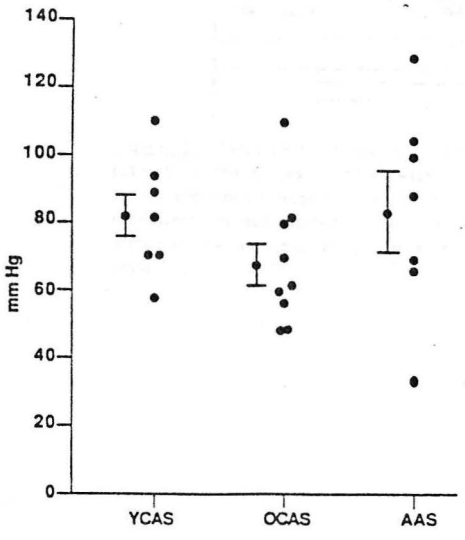

Figure 10. Peak aortic valve pressure gradients in the three groups of patients with aortic stenosis. The group gradients are not statistically different. (Assey et al., 1987).

Left ventricular mass (normalized to body surface area) was elevated in all three patient groups. However, the magnitude of enlargement was greater in both young patient groups compared to the adult patients.

Ejection fractions for the experimental and control groups are shown. Ejection fractions for the two young groups with aortic stenosis were significantly higher than their age matched controls, while adults with aortic stenosis had ejection fractions similar to their control group.

Figure 11.

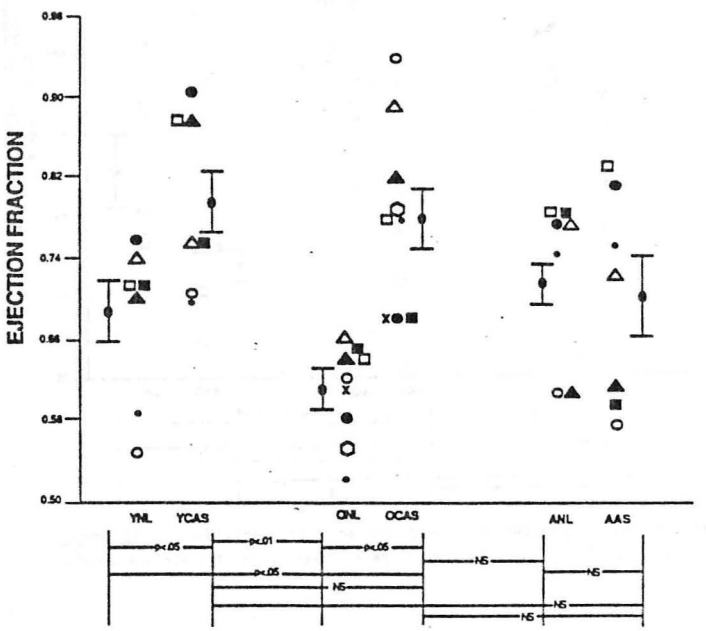

Figure 11. Ejection fractions (EFs) for the six groups of patients. Each patient in the groups of those with aortic stenosis is represented by a symbol and the corresponding symbol for each subject in the control group represents the age-matched control for that patient. The comparisons were performed by analysis of variance followed by the Newman-Keuls test. (Assey et al., 1987).

Wall stress was significantly lower in the young aortic stenosis groups compared to their controls, whereas it was identical in the adult group.

Figure 12.

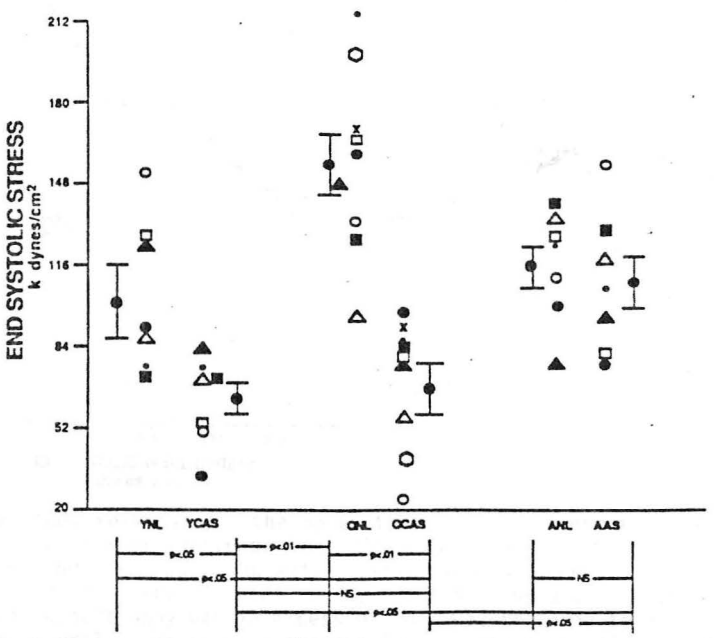

Figure 12. Wall stress for the six groups of patients. Symbols are matched and statistical analysis is as in figure 11. (Assey et al., 1987).

The inverse relationship between ejection fraction and wall stress for all patients and controls is demonstrated.

Figure 13.

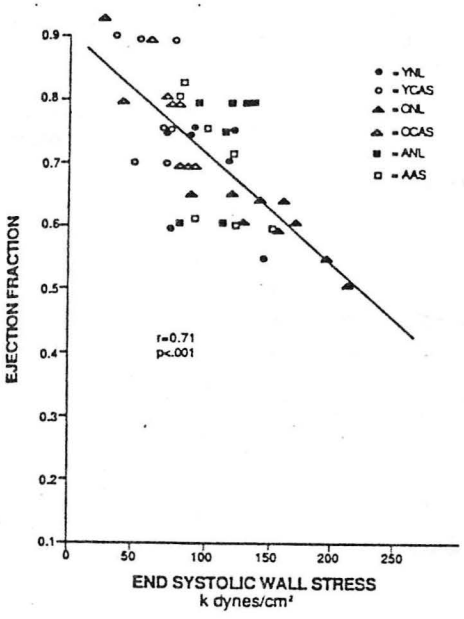

Figure 13. Ejection fraction plotted against end-systolic wall stress for the six groups of subjects. The figure demonstrates that patients with congenital aortic stenosis had higher ejection fractions and lower wall stress than control subjects. There is a linear correlation between ejection fraction and wall stress, as shown throughout the range of the variables. (Assey et al., 1987).

This study reemphasizes the point that if wall stress remains normal in the face of increased workload, then the usual clinical measures of overall ventricular function remain normal. Maintenance of normal wall stress has been suggested to be the stimulus for hypertrophy. However, in the two groups of children, hypertrophy was in excess of what was required to maintain normal wall stress - wall stresses were abnormally low, while ejection fractions were supernormal (Assey et al., 1987). It is unclear whether this represents a more extensive hypertrophic response in children or a limited hypertrophic response in the adult.

The above cited clinical studies would suggest that if the tissue response to increased workload is quantitatively sufficient to maintain wall stress at normal levels, then overall cardiac function is benefitted by the hypertrophy process. By contrast, Huber et al. (1981) and Spann et al. (1980) studied patients with aortic stenosis and found that wall stress could be normal in patients with depressed ejection fractions. Huber (1981) further demonstrated that in patients with normal wall stress, contractility might nonetheless be impaired, suggesting that qualitative abnormalities exist in hypertrophied, compensated myocardium. Takahashi et al. (1980) made similar observations in a group of patients with hypertrophy resulting from systemic hypertension, all of whom had normal overall left ventricular function.

Studies which examine function of isolated muscle strips from animals with hypertrophy but preserved systolic function have found substantial intrinsic abnormalities of muscle function. Spann et al. (1967) using a feline model of right ventricular hypertrophy induced by pulmonary artery

banding, studied normal control animals and animals with right ventricular hypertrophy without evidence of failure as well as with failure. In those animals with hypertrophy but without congestive heart failure, there were significant alterations in the following parameters of muscle function.

The relationship between fiber length and active tension generation was shifted downward and to the right so that for any given muscle length, tension generated was significantly decreased in hypertrophied fibers.

Figure 14.

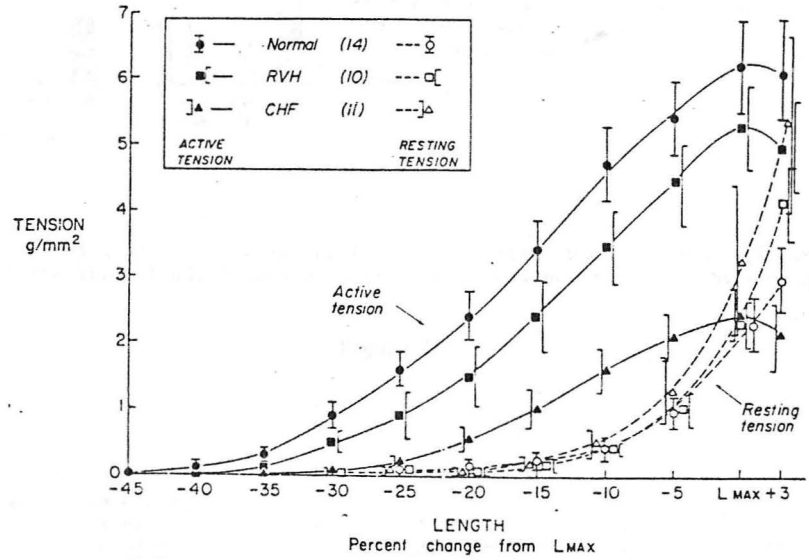

Figure 14. Relation between muscle length and tension of the papillary muscles from normal (circles), hypertrophied (squares) and failing (triangles) right ventricles. Open symbols=resting tension; solid symbols=actively developed tension. Each value is the average of the group; vertical lines with cross bars = ±1 SEM. Tension is corrected for cross-sectional area (g/mm^2). Numbers in parentheses=number of animals. (Spann et al., 1967).

Rate of maximum isometric force development was depressed.

Figure 15.

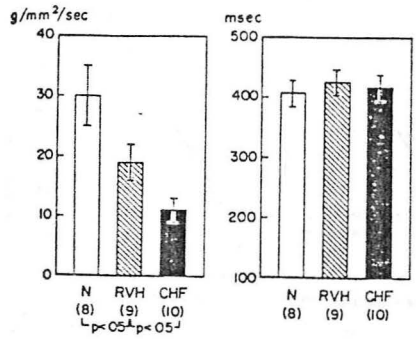

Figure 15. Left, maximum rate of isometric force development shown for the three groups of muscles in $g/mm^2/sec$. All muscles were studied at the apex of their length-tension curves. Right, time from stimulation to the peak of developed isometric tension in milliseconds. All muscles were studied at the apex of their length-tension curves. Numbers in parentheses=number of animals. Vertical lines with cross bars = ±1 SEM. (Spann et al., 1967).

The force-velocity relationship was shifted downward and leftward so that at any given load, velocity of shortening was depressed for hypertrophied fibers.

Figure 16.

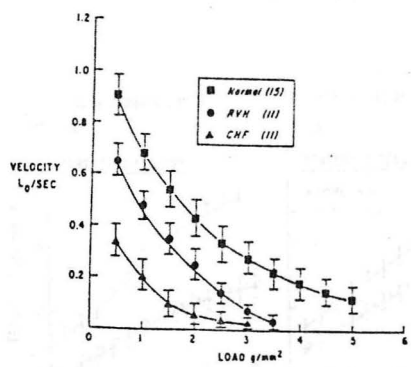

Figure 16. The force-velocity relations of the three groups of cat papillary muscles. Average values with ± SEM are given for each point. Velocity has been corrected to muscle lengths per second (L_o/sec). Numbers in parentheses=number of animals. (Spann et al., 1967).

Capasso et al. (1981) using a model of renal hypertension and hypertrophied left ventricular papillary muscles from rats also found that velocity of shortening was impaired by 10 weeks of hypertension but found developed tension in hypertensives to be significantly greater than control animals.

Figure 17.

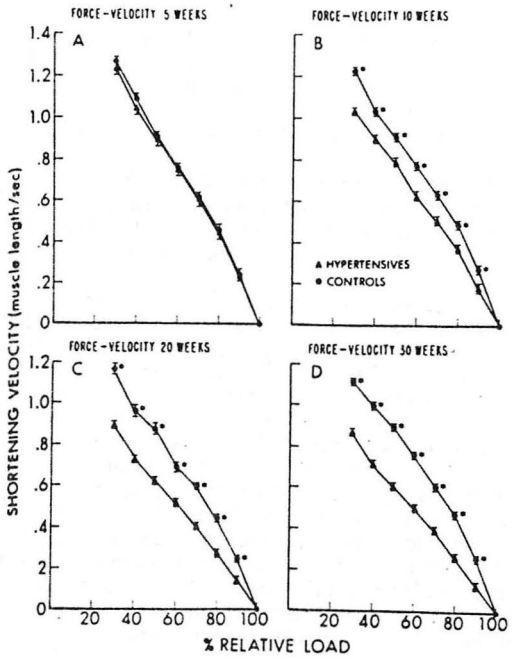

Figure 17. Normalized force-velocity relations at bath $[Ca^{2+}]$ 2.4 mM. Values were obtained from a series of afterloaded isotonic contractions at an initial muscle length of L_{max}. Force is expressed as % relative load (total isotonic load/total isometric load X 100). Velocity is expressed as number of muscle lengths per second, calculated as peak velocity (in mm/s) divided by L_{max}. Values are plotted as means ± SE. Velocities were significantly lower in hypertensives than controls in each study. *$P \leq 0.05$. A: 5 wk hypertension (closed triangles, hypertensives; closed circles, controls; n=12). B: 10 wk hypertension (closed triangles, hypertensives; closed circles, controls; n=10). C: 20 wk hypertension (closed triangles, hypertensives; closed circles, controls; n=11). D: 30 wk hypertension (closed triangles, hypertensives; closed circles, controls; n=10). (Capasso et al., 1981).

Figure 18.

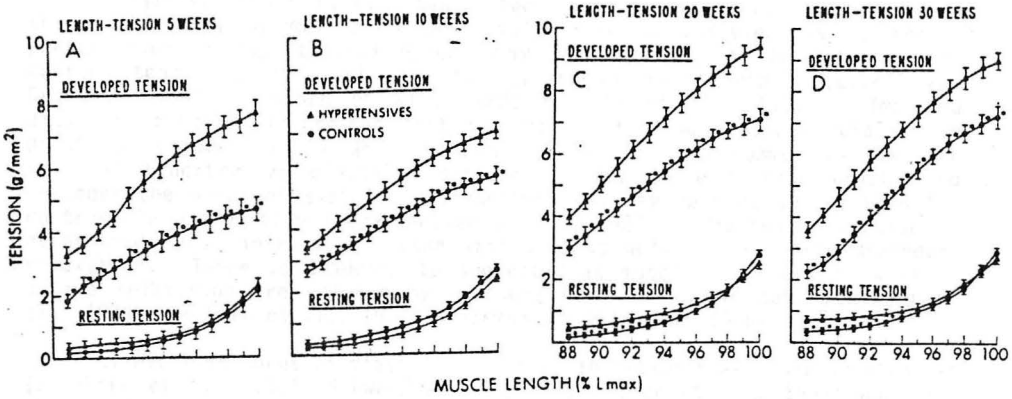

Figure 18. Resting and developed tensions are plotted as a function of muscle length in hypertensives and controls. Bath $[Ca^{2+}]$ 2.4 mM. Values are plotted as means ± SE. *P, ≤ 0.05. A: 5 wk hypertension (closed triangles, hypertensives; closed circles, controls; n=12). B: 10 wk hypertension (closed triangles, hypertensives; closed circles, controls; n=10). C: 20 wk hypertension (closed triangles, hypertensives; closed circles, controls; n=11). D: 30 wk hypertension (closed triangles, hypertensives; closed circles, controls; n=10). (Capasso et al., 1981).

Time to peak tension was measured in this study and was found to be prolonged.

Jouannot (1975), using aortic banded rats found that time to peak tension was prolonged and the muscle developed length-tension relationship was depressed. While there is some variability in the peak tension generated relative to control, prolongation of time to peak tension is uniformly described in hypertrophied myocardium.

Information on intrinsic muscle function is not available from patients with stable compensated hypertrophy; however, these animal studies would suggest that despite preservation of overall ventricular function, function of individual myocardial units is impaired.

One important objection to many of the animal studies of hypertrophy is that usually a sudden large afterload is imposed and the duration of the afterload increase is substantially shorter than would be found clinically. It has been shown (Sasayama et al., 1976,1977) that associated with sudden imposition of increased afterload, there is transient depression of overall function as measured by ejection fraction and velocity of muscle fiber shortening, with subsequent recovery of overall function. Carabello et al. (1981) used the opposite approach and studied overall function during gradual imposition of pressure load created by banding puppies with a non-constricting aortic band which became constricting as the puppies matured. Ejection fraction, rate of pressure development and velocity of muscle fiber shortening were serially compared with a group of sham-operated litter mate controls. The two groups were functionally indistinguishable at all time points. However, it should be reemphasized that measures of overall ventricular function are not necessarily reflective of intrinsic muscle function.

Diastolic Function.

Congestive heart failure manifested by pulmonary venous congestion in the setting of normal or supernormal systolic function is a common presentation in hypertensive hypertrophy, as well as in the patient with aortic stenosis particularly in the setting of an arrhythmia (Lorell and Grossman, 1987; Eichhorn et al., 1982; Hanrath et al., 1980). Impaired diastolic function (increased left ventricular filling pressure relative to diastolic volume (Lorell and Grossman, 1987)) is very common in pressure overload hypertrophy; diastolic dysfunction may be a finding which long precedes the onset of systolic dysfunction, and may be more severe than the contractile dysfunction (Lecarpentier et al., 1987). Diastolic function is determined by 1) intrinsive tissue stiffness as well as 2) energy dependent relaxation. There is evidence to suggest that muscle stiffness as well as active relaxation are altered by pressure overload hypertrophy (Schwarz et al., 1978; Eichhorn et al., 1982; Grossman and McLaurin, 1976).

Clinical measures of diastolic function in patients with aortic stenosis (Eichhorn et al., 1982; Schwarz et al., 1978; Fifer et al., 1985) and with chronic hypertension (Hanrath, 1980) all show abnormalities in ventricular filling. Eichhorn et al. (1982) found the time constant of decay of left ventricular pressure was prolonged in 13 patients with aortic stenosis (67 msec vs 41 msec, $p<0.01$) and normal systolic function. The time constant did not correlate with left ventricular systolic pressure, but did significantly

correlate with ventricular mass. Fifer et al. (1985) measured rates of left ventricular early diastolic filling and wall thinning in both children and adults with aortic stenosis, and found these indices to be depressed in both patient groups when compared to normal controls. Importantly, depression of diastolic function was noted in children with supernormal systolic function as well as low wall stress. Schwarz et al. compared the degree of diastolic dysfunction to morphologic abnormalities of increased myofiber diameter as well as fibrosis in patients before and after aortic valve replacement. Interestingly, diastolic dysfunction was best correlated to muscle cell diameter rather than fibrosis, suggesting that the component of diastolic dysfunction attributable to passive elastic properties of the myocardium were dependent upon the myocardial cell, rather than upon the increased collagen content.

In addition to changes in myocardial stiffness (Schwarz et al., 1978), there is considerable evidence that active relaxation is also impaired. Studies of isolated muscle fibers show that the rate of isometric relaxation is decreased (Jouannot, 1975), the time to half relaxation is prolonged (Capasso et al., 1981; Lecarpentier et al., 1987). An important finding of Lecarpentier et al. was the disappearance of load sensitivity of relaxation in severely hypertrophied myocardium. This property is present when sarcoplasmic reticulum is present and normally functional, and not present under conditions when sarcoplasmic reticulum is either not present or pharmacologically inhibited. Gwathmey et al. (1985) present further evidence that calcium uptake by sarcoplasmic reticulum in hypertrophied myofibers is disturbed. In summary, changes in passive muscle stiffness as well as impaired active relaxation probably contribute to the diastolic dysfunction observed in hypertrophied myocardium.

Excitation - Contraction Coupling

While peak tension generated by hypertrophied myocardium may be somewhat variable, the prolongation in the time to peak tension is relatively constant. There is a corresponding change in the excitation-contraction coupling which is thought to be responsible for the prolongation of contraction. Normal excitation-contraction coupling is shown below.

Figure 19.

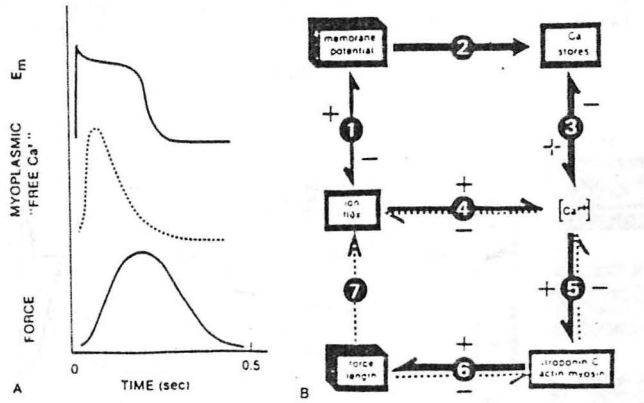

Figure 19. A, Schematic illustration of the approximate time course of excitation-activation-contraction coupling. From top to bottom, the transients are the cell membrane action potential, the myoplasmic $[Ca^{++}]$ as measured by the photoprotein aequorin, and myocardial force developed during an isometric contraction. Note the sequence of events: the action potential precedes the rise in myoplasmic free $[Ca^{++}]$, which in turn precedes the onset of force development. The decline in myoplasmic $[Ca^{++}]$ precedes the fall-off in force. B, Schematic diagram of some interactions between membrane potential and contraction in the heart. The sequence in excitation-activation-contraction coupling may be followed via the heavy black arrows (mainly clockwise). Ion fluxes across the sarcolemma [arrow 1+] determine the membrane potential, which itself can provide a driving force for ion movements [arrow 1-]. The changes in membrane potential are a function of the ionic equilibrium potentials and conductances. The depolarization [2] causes a rise in myoplasmic $[Ca^{++}]$ derived from intracellular stores [3+]. This results directly from the depolarization or possibly from Ca^{++}-induced Ca^{++} release. The Ca^{++} within the myoplasm combines with troponin C[5+] to allow an actin-myosin interaction requiring ATP and resulting in force development [6+]. At the time that, or probably before, the membrane repolarizes, the sarcoplasmic reticulum sequesters Ca^{++}[5-; 3-] permitting relaxation to occur [6-]. Ca^{++} can also leave the myoplasm by a metabolically dependent Ca^{++} pump or by Na^{+}, Ca^{++}-exchange [4-]. Force and length changes could influence membrane events (contraction-activation-excitation feedback) by processes depicted the dotted lines. For example, these mechanical alterations could change ionic fluxes across the sarcolemma by affecting permeability or diffusion gradients directly [7]. Indirectly, force and length changes could influence the membrane by altering myoplasmic $[Ca^{++}]$[6-; 5-]. This may influence ionic flux [4-], and hence, membrane potential [1+] by modulation of the electrochemical gradient for Ca^{++} and thus, modulation of the slow Ca^{++} channel, outward K^{+} currents, "leak" currents, the electrogenic Na^{+}/Ca^{++} exchange, or the nonspecific cation conductance referred to as the oscillatory or transient inward (TI) current. (Braunwald et al., 1988).

In hypertrophied muscle, the action potential is prolonged with a corresponding prolongation of the time course of tension generation. Of interest, both action potential duration and the time course of tension generation normalize with regression of hypertrophy (Capasso et al., 1982).

Figure 20.

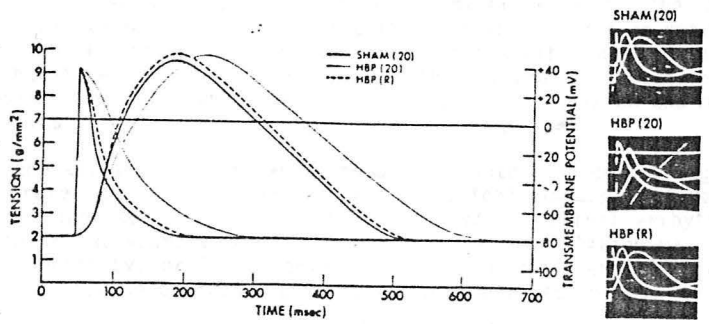

Figure 20. Superimposed tracings of oscilloscopic photographic records of isometric tension and action potentials from SHAM (20), HBP (20), and HBP (R) papillary muscles. Insert shows actual oscilloscopic records from SHAM (20), HBP (20), and HBP (R) papillary muscles. (Capasso, 1982).

Left Ventricular Hypertrophy and Arrhythmias

The presence of left ventricular hypertrophy by electrocardiogram and more recently echocardiogram has been associated with a three to five-fold increased likelihood of sudden death (Kannel et al., 1975). Of interest, this increased incidence of sudden death is in excess of the risk of sudden death associated with the presence of hypertension alone (Kannel et al., 1975) suggesting an independent contribution to the risk for sudden death made by the presence of hypertrophy. Thus for men in the Framingham-Albany cohort, hypertension increased the risk of sudden death three-fold, while electrocardiographic evidence of left ventricular hypertrophy increased the risk five-fold. While this is of interest, it does not clearly show that hypertrophy is the precipitant to sudden arrhythmic death - one might postulate, for example, that left ventricular hypertrophy (stimulated by myocardial ischemia) was associated with more severe coronary artery disease, and thus, the severity of the coronary disease, rather than hypertrophy per se might be responsible for the increased incidence of sudden death. Perper et al. (1975), however, found no correlation between heart weight and severity of coronary artery disease in patients dying suddenly thus, countering the argument that hypertrophy is simply another consequence of the disease process producing increased sudden death. In a somewhat different setting, Messerli et al. (1984) quantitated ventricular ectopic activity in patients with hypertension with and without hypertrophy. The authors noted that patients

with hypertension, but without hypertrophy had ventricular ectopic activity no different than normal control subjects; however, if hypertrophy was present in addition to hypertension, ventricular ectopic activity was significantly increased. Importantly, coronary artery disease was excluded in this group of patients.

Further evidence that hypertrophy independent of coronary artery disease may provide a proarrhythmic substrate is suggested by the fact that other diseases associated with pressure overload hypertrophy in the absence of coronary artery disease, such as aortic stenosis in children or coarctation of the aorta, are associated with sudden arrhythmic death (Jones et al., 1980). It is, therefore, worth considering whether there are features of the hypertrophied myocardium which might potentiate the initiation and maintenance of arrhythmias.

In general, arrhythmias can be subdivided into disorders of automaticity (abnormal rate, or site of origin of electrical impulse generation) and disorders of impulse conduction (Cranefield, 1973). Lethal arrhythmias such as ventricular tachycardia leading to ventricular fibrillation may arise from altered automaticity, or from reentry secondary to differential conduction of an electrical impulse or from a combination of these mechanisms.

There is substantial data showing that electrophysiologic alterations exist in compensated, non-ischemic hypertrophied myocardium which could provide the substrate for the initiation and maintenance of arrhythmias.

The normal action potential consists of changes in membrane voltage determined by transmembrane ionic currents. These are summarized on the diagram below. Current passes from cell to cell in an orderly fashion and results in mechanical activation of myocytes.

Figure 21.

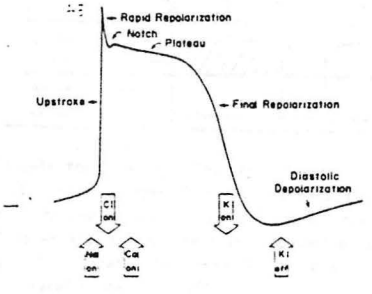

Figure 21. Diagrammatic representation of a cardiac action potential, emphasizing characteristics of the Purkinje fiber. Upstroke is phase 0; rapid repolarization is phase 1; plateau is phase 2; final repolarization is phase 3; and diastolic depolarization if phase 4. The arrows below the diagram refer to the approximate time when the indicated ion is influencing membrane potential. They point in the direction of the effect on the membrane potential, upward for depolarization and downward for repolarization. (Fozzard, 1977).

Many myocardial cells possess the ability to spontaneously depolarize and generate an action potential (automaticity). Arrhythmias resulting from altered automaticity arise when some factor enhances the spontaneous electrical activity of one or more of the latent myocardial pacemakers. When this occurs a single ectopic or a sustained ectopic arrhythmia may result. Reentrant arrhythmias, by contrast, occur when there is a localized area of abnormal conduction slowing such that an impulse traveling this circuit is delayed sufficiently at one point that it reaches tissue which would normally be refractory to excitation but is excitable due to the impulse delay, and is thus capable of generating a single or series of ectopic beats (Cranefield, 1973).

Figure 22.

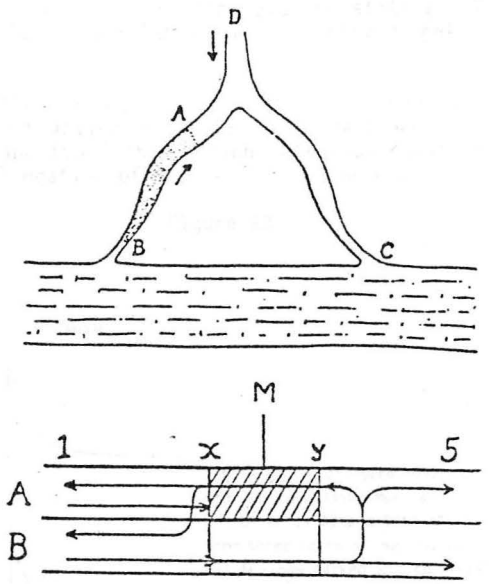

Figure 22. Models for reentry. The upper figure consists of a Purkinje fiber bundle (D) which divides into two branches (B and C). These two branches are connected distally by ventricular muscle. The stippled segment (A-B) is an area of unidirectional conduction block. In the lower figure A and B indicate two parallel muscle fibers with lateral connections. (Cranefield et al., 1973).

In practice, clear separation of arrhythmias into these two mechanisms is not feasible and arrhythmias may result from a combination of both mechanisms. Importantly, it can be shown that the substrate for both mechanisms of arrhythmogenesis exist in hypertrophied myocardium.

Cameron et al. (1983) using a model of aortic constriction with resultant LV hypertrophy, found abnormalities in action potential duration, upstroke velocity and amplitude of the action potential that were heterogeneous within the same heart. In some regions of the heart, action potentials were shortened with low upstroke velocity and low amplitude, while in other regions action potentials were prolonged. Conduction velocity of electrophysiologic impulses are directly related to upstroke velocity so that areas of low upstroke velocity would create regions of conduction delay. Electrocardiographic monitoring was done with and without vagal stimulation to slow heart rate in hypertrophied and control animals. When heart rate was slowed, arrhythmias including single and repetitive PVC's as well as spontaneous ventricular fibrillation were observed only in hypertrophied hearts.

Aronson (1980), using microelectrode techniques, studied the characteristics of the action potential from rats with renal hypertension-induced hypertrophy and found that action potential duration was increased as a consequence of prolongation of the refractory period.

Figure 23.

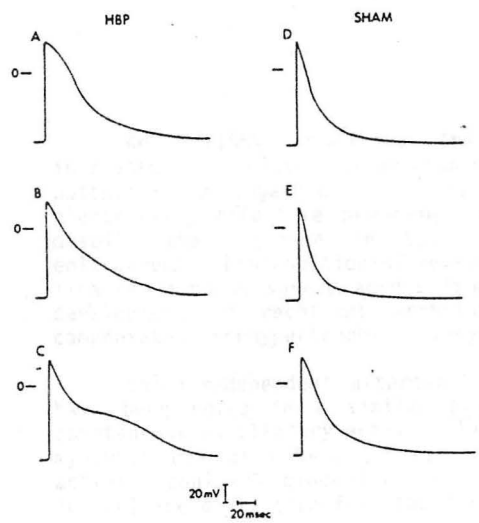

Figure 23. Configurations of representative AP recorded from the papillary muscles of SHAM and HBP rats. Traces of HBP AP (A-C) and SHAM AP (D-F) recorded simultaneously from three pairs of muscles taken from animals. Note that HBP AP show marked and consistent lengthening as well as considerable variability in the course of repolarization. Horizontal bars show zero potential. (Aronson, 1980).

Keung and Aronson (1981) found that the prolongation of refractoriness was distributed in a non-uniform fashion among endocardial, epicardial and papillary muscle segments; such nonuniformity would provide areas of conduction delay.

Figure 24.

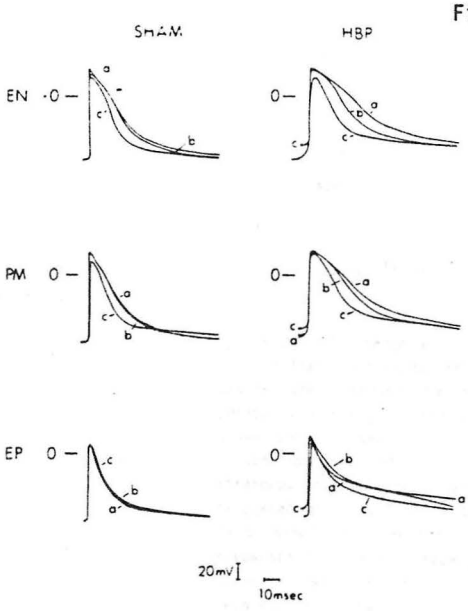

Figure 24. Tracings of representative action potentials showing the effect of DCL on configuration. DCL=1000 (a), 300 (b) and 150 (c) msec. Tracings are from endocardial (EN), papillary muscle (PM), and epicardial (EP) fibers of SHAM and HBP rats. Note that HBP action potentials of endocardial and papillary muscle fibers are clearly longer than those of SHAM fibers at longer DCL. Prolongation of epicardial HBP action potentials is seen only during the latter half of repolarization. (Keung and Aronson, 1981).

Keung (1989) found that the transmembrane inward calcium current was increased in isolated hypertrophied myocytes and accounted for the action potential prolongation. It has also been reported that the amount of electrically effective membrane area is reduced in hypertrophied myocardium despite the increase in total membrane area resulting from cellular enlargement. Prolongation of refractoriness, dispersal of refractoriness, and impaired impulse spread across from cell to cell are the substrates for the development of reentrant arrhythmias and have been found to exist in compensated, nonhypertrophied myocytes.

Calcium-dependent afterdepolarizations resulting in triggered activity have been noted in a similar preparation (Aronson, 1981). Additionally, spontaneous oscillatory activity leading to action potentials in hypertrophied myocytes has also been noted. Of interest, this spontaneous oscillatory activity could be blocked by caffeine, a substance which blocks both uptake and release of calcium from the sarcoplasmic reticulum.

Figure 25.

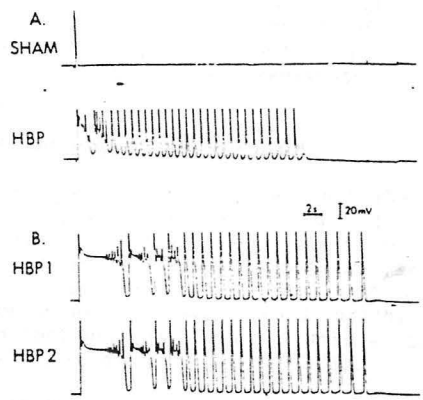

Figure 25. Triggered activity arising from early afterdepolarizations in HBP papillary muscles exposed to TEA. In A, the same external stimulus was applied simultaneously to the SHAM and HBP muscles following a quiescent period of 2 minutes. The SHAM preparations responded with only a single drive action potential whereas the repolarization phase of the driven action potential of the HBP preparation was interrupted by an early afterdepolarization that gave rise to sustained triggered activity; the triggered activity finally terminates with a delayed afterdepolarization. In B, simultaneous recording were obtained from 2 sites in the same HBP preparation (interelectrode distance, 1.5 mm). A single drive action potential was evoked after a quiescent period of 2 minutes. The repolarization phase of the driven action potential is interrupted by an early afterdepolarization which, after an initial quiescent period, gives rise to progressively larger oscillatory responses. The first burst of this triggered oscillatory activity ceases when the membrane repolarizes to a negative level, but then a spontaneous upstroke occurs, apparently from the depolarizing phase of a delayed afterdepolarization. The repolarization phase of this action potential is again interrupted by oscillatory triggered activity. This same sequence is repeated twice more until the membrane potential following repolarization of the fourth burst of oscillatory activity remains at negative levels of membrane potential but sustained spontaneous activity follows, presumably having arisen from the depolarizing phase of a delayed afterdepolarization. The diastolic membrane potential attains gradually more negative levels with each subsequent beat until spontaneous activity terminates with a small and slow delayed afterdepolarization. Note that the electrical activity recorded at both sites is synchronous. This is an example of triggered activity initiated by the alternation of early and delayed afterdepolarizations. (Aronson, 1981).

Thus in nonischemic hypertrophied myocardium, prolongation and dispersal of refractoriness, as well as heterogeneity of conduction velocity have been identified, and may facilitate the development of reentrant arrhythmias. Alternatively, the presence of calcium-dependent after potentials which may lead to triggered electrical activity may predispose to arrhythmias secondary to altered automaticity.

Hypertrophy and the Coronary Circulation

Two clinical observations have suggested that the coronary circulation may be abnormal in hypertrophied myocardium. Angina pectoris, in the absence of atherosclerosis in the epicardial coronary arteries, occurs as a major symptom in aortic stenosis (Marcus et al., 1982) and may also be observed in patients with hypertension and hypertrophy (Brush et al., 1988). Patients with hypertrophy undergoing exercise electrocardiography may have abnormal ST segment responses consistent with ischemia, as well as angina in the absence of obstructive coronary artery disease (Brush, 1988).

Anatomic studies of the coronary vasculature in both humans and animals have shown that the epicardial coronary arteries enlarge with hypertrophy (Marcus et al., 1987); the enlargement, however, is not proportional to the amount of hypertrophy, and these arteries constitute only a small proportion of the overall cross-sectional area of the coronary vasculature. Morphometry of the coronary microcirculation (which constitutes the largest cross-sectional area of vasculature) has shown that the capillary density is decreased by 20-30% in the pressure overloaded heart (Rakusan et al., 1980; Holtz et al., 1977) thus, suggesting that growth of the major portion of the coronary vasculature is not commensurate with the growth in myocardial mass. A different method of measuring the amount of microcirculation is to functionally assess the cross-sectional area of the capillary bed by calculation of coronary vascular resistance (pressure drop across the coronary circulation (mmHg) ÷ mean coronary blood flow (ml/min) across the coronary circulation during maximal, pharmacologic vasodilation (to ensure that all vascular channels are open); this quantity, the minimal coronary vascular resistance, is linearly related to the cross-sectional area of the coronary bed. One can then calculate the resistance per gram of tissue to normalize for increases in myocardial mass. If the coronary microvascular growth is equivalent to the increased muscle mass, then for any given pressure drop, the coronary flow rate should increase, resulting in a decrease in overall resistance and no change in resistance per gram of myocardium. In hypertrophied myocardium resulting from renal hypertension (Mueller et al., (1978) and from aortic banding (O'Keefe et al., 1978), calculation of the minimal vascular resistance per gram of myocardium has shown that minimal coronary vascular resistance per gram of tissue was significantly increased in both models of hypertrophy, indicating a decrease in the functional cross-sectional area of the coronary capillary bed.

Figure 26.

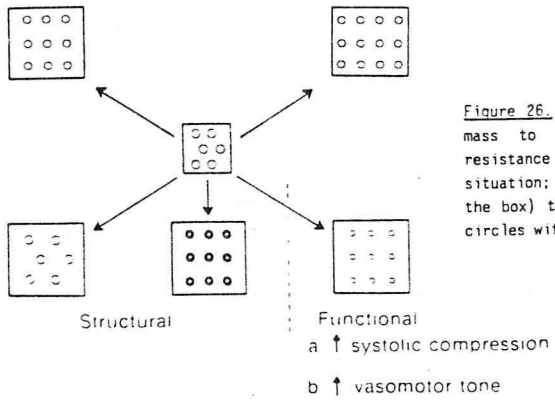

Figure 26. Conceptual diagram which relates ventricular mass to the cross-sectional area of the coronary resistance vessels. The center box reflects the normal situation; i.e., the ratio of ventricular mass (size of the box) to size of the vascular bed (total area of the circles within the box) is normal. (Marcus, 1983b).

The above diagram adapted from Marcus (1983b) illustrates the anatomic changes accompanying pressure overload hypertrophy. The relationship between normal microvasculature and myocardial mass is shown as the center square. The bottom left square illustrates the failure of the coronary circulation to increase with muscle mass, the bottom center square shows an increase in vasculature which is structurally abnormal leading to increased vascular resistance across the whole heart, while the bottom right panel shows increased microvasculature which is functionally subject to elevated compressive forces (i.e. increased end-diastolic pressure), and thus extrinsically compressed resulting in elevated resistance.

Hypertrophy has also been found to be associated with significant alterations in the regional distribution of blood flow resulting in selective underperfusion of the subendocardium. Under normal circumstances, the endocardial blood flow is larger than epicardial blood flow resulting in a endocardial to epicardial blood flow ratio significantly greater than 1.0. Bache et al. (1981) compared the endocardial to epicardial flow gradients in normal dogs, and those with hypertrophy, and found the following: At rest in normal dogs, subendocardial flow significantly exceeded subepicardial flow, the (endo:epi blood flow ratio was 1.25±0.07) while in hypertrophied hearts, this ratio was 1.1±0.08, so that endocardial flow was not significantly different from epicardial. With exercise, flow increased linearly with increasing workload in all groups, with a relative redistribution of blood flow away from the subendocardium in all groups; however, the endo- to epi-blood flow ratios significantly decreased in hypertrophied versus normal hearts (endo:epi ratio 0.94±0.03 in LVH vs 1.10±0.08 in normal hearts, $p<0.05$).

Figure 27.

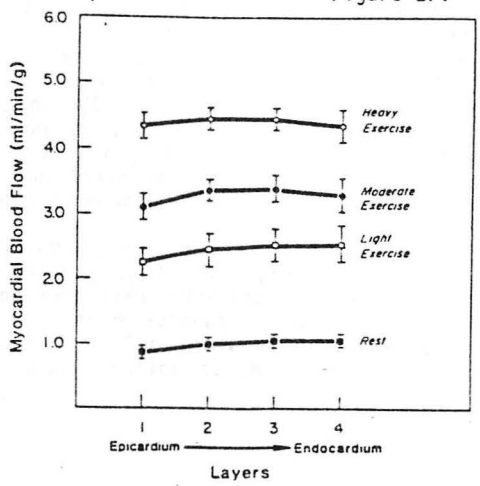

Figure 27. Mean left ventricular myocardial blood flow (ml/min per g) ± SEM to four transmural layers measured at rest and during three levels of treadmill exercise in nine normal control dogs. (Bache et al., 1981).

Figure 28.

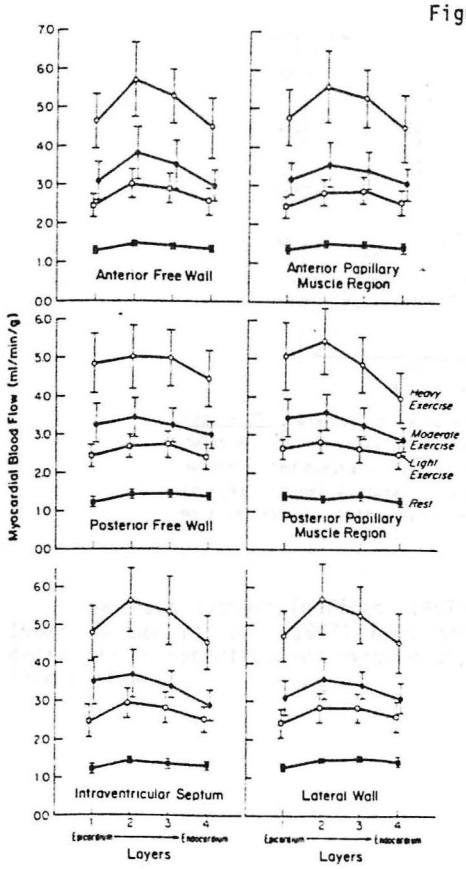

Figure 28. Mean left ventricular myocardial blood flow (ml/min per g) ± SEM to each of the six circumferential regions and four transmural layers measured at rest and during three levels of treadmill exercise in eight dogs with left ventricular hypertrophy. (Bache et al., 1981).

Using a similar model, Vrobel et al. (1980) showed that incremental pacing of normal and hypertrophied hearts resulted in no change in the regional distribution of blood flow in the normal animals, but a significant redistribution of blood away from the subendocardium at maximal heart rates of 250 beats/minute (endo:epi flow ratio 1.03±0.08 at 100/min versus 0.83±0.06 at 250/min, $p<0.05$, in hypertrophied hearts, endo:epi flow ratio 1.08±0.03 at 100/min versus 1.02±0.05 at 250/min, p=NS, in normal dogs). Because the subendocardial region is the area of greatest wall tension and as well as highest metabolic activity, redistribution of blood flow with stress in hypertrophied hearts is clearly disadvantageous.

An important property of the coronary circulation is autoregulation of flow - the ability to maintain constant flow under widely variable coronary perfusion pressures (Hoffman, 1987). If maximal coronary vasodilation is accomplished then autoregulation is lost and coronary flow varies linearly with pressure. The difference between autoregulated flow and flow during maximal vasodilatation at any given perfusion pressure is the coronary flow reserve.

Figure 29.

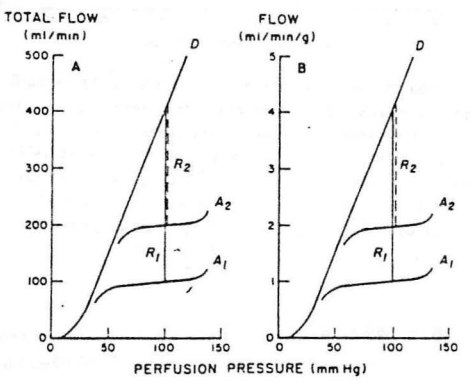

Figure 29. Diagram of basic coronary flow reserve. D = pressure flow relation during maximal vasodilatation; A_1, A_2 = two levels of autoregulated coronary flow; R_1 = flow reserve from A_1; R_2 = flow reserve from A_2. Panel A, Total flow per ventricle (ml/min); B, flow per unit mass (ml/min/g). Left ventricular weight, 100 g. (Hoffman, 1987).

Numerous authors (Hoffman, 1987; Murray and Vatner, 1981; Marcus et al., 1982; Marcus et al., 1987) have shown that the coronary flow reserve is decreased in hypertrophied myocardium. This is very nicely shown in this data from Hoffman.

Figure 30.

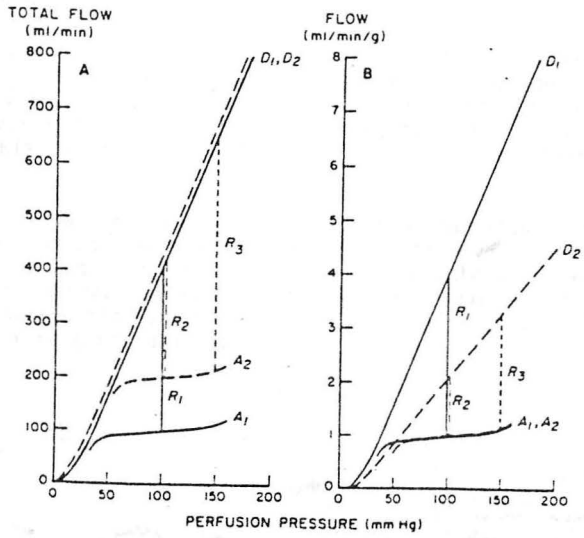

Figure 30. Diagram of coronary flow reserve with hypertrophy. Pressure-flow relationships for normal left ventricle (100g) and hypertrophied left ventricle (200 g). A = autoregulated flows; D = pressure flow line during maximal vasodilatation; R = flow reserve. Normal: A_1, D_1, R_1, and solid lines; hypertrophied: A_2, D_2, R_2, R_3, and dashed lines. D_1 and D_2 are superimposed. Reserve for hypertrophied ventricles is shown at normal (R_2) and elevated (R_3) perfusing pressure. A, Total flow per ventricle; B, flow per unit mass. (Hoffman, 1987).

Coronary reserve is diminished because the flow per gram of tissue during maximal vasodilation tissue is decreased.

Figure 31.

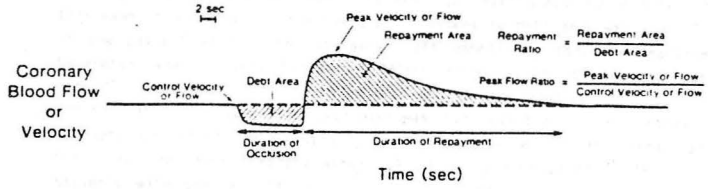

Figure 31. Standard measurements used to analyze reactive hyperemic responses. (Marcus, 1983b).

Another way to assess flow reserve is to occlude a coronary artery for 10-20 seconds then measure the hyperemic response (transient increase in blood flow following release of coronary occlusion which is metabolically determined) (Murray and Vatner, 1981).

Calculation of the ratio of the area under the hyperemic flow curve (repayment area) to the area under the occlusion period (debt area) generates a ratio of debt to occlusion area which quantifies the hyperemic response. In normal, nonhypertrophied dogs this ratio is about 4:1. In the presence of hypertrophy this response is significantly attenuated (Murray and Vatner, 1981).

Coronary flow reserve assessed by the magnitude of the reactive hyperemic response has been quantified in patients with aortic stenosis at the time of surgery, and found to be significantly attenuated when compared to nonhypertrophied subjects (Marcus, 1982). The repayment area to debt area ratio in nonhypertrophied subjects was approximately 3.6:1 compared to a ratio of 1:1 for hypertrophied subjects.

Figure 32.

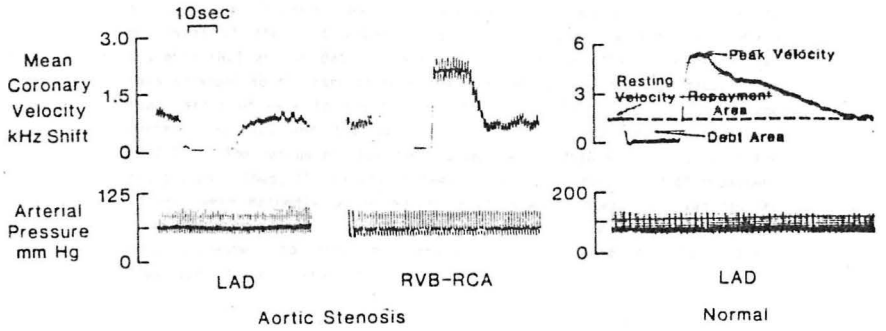

Figure 32. Coronary Reactive Hyperemia Responses in a Patient with Aortic Stenosis and in a Control. Recordings of mean coronary velocity are shown in the top panels, and recordings of arterial pressure in the bottom panels. A 20-second occlusion of the coronary arteries had no significant effect on aortic pressure, heart rate, or cardiac rhythm. In the control patient (right panel) release of a 20-second occlusion of the left anterior descending (LAD) coronary artery was followed by a marked increase in the velocity of coronary blood flow. The ratio of peak to resting velocity in this example was about 4; the ratio of repayment to debt area was about 3. In the patient with aortic stenosis (left panel) the coronary reactive hyperemia response that followed a 20-second occlusion of the LAD was markedly attenuated. The ratio of peak to resting velocity was about 1, and the ratio of repayment to debt area was much less than 1. In contrast, the same patient had an essentially normal response in a right ventricular branch of the right coronary artery (RVB-RCA) (center panel). Thus, in patients with severe left ventricular hypertrophy secondary to valvular aortic stenosis, coronary reserve - assessed by measuring the quantitative characteristics of coronary reactive hyperemia - is markedly decreased in the coronary vessels that supply the hypertrophied ventricle. (Marcus et al., 1982).

The ratios of peak to baseline blood flow velocity was 4.6:1 in normals compared to 1.9:1 for hypertrophied subjects.

Figure 33.

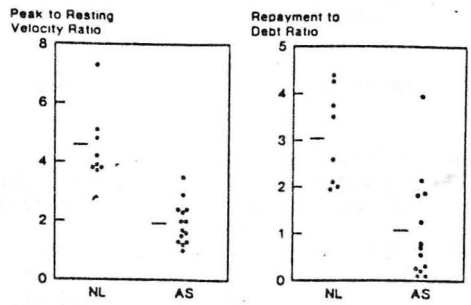

Figure 33. Ratios of peak to resting velocity and of repayment to debt area in the coronary reactive hyperemia responses (after a 20-second occlusion of the left anterior descending coronary artery) in control patients (NL) and in patients with aortic stenosis (AS). The horizontal bars adjacent to the circles represent the mean values for each group. The mean ratios of peak to resting velocity were 4.6±0.4 and 1.9±0.2 in the control patients and the patients with aortic stenosis, respectively ($P<0.01$). The ratios of repayment to debt was 3.05±0.4 and 1.1±0.3 in the two groups. Thus, the ratios of peak to resting velocity and of repayment to debt were markedly decreased in patients with severe left ventricular hypertrophy secondary to aortic stenosis. Only 13 dots are shown in the AS group (repayment to debt area) because two points were identical and are thus superimposed. (Marcus et al., 1982).

In summary, ventricular hypertrophy in response to pressure overload results in increased muscle mass, normalization of wall stress and preservation of cardiac output. The biologic consequences of maintenance of normal contractile function, include diminished diastolic compliance, electrophysiologic changes which may potentiate arrhythmogenesis and alterations in the coronary circulation favoring subendocardial ischemia as well as diminished coronary reserve.

REFERENCES

Alpert NR, Mulieri LA: Increased myothermal economy of isometric force generation in compensated cardiac hypertrophy induced by pulmonary artery constriction in the rabbit. A characterization of heat liberation in normal and hypertrophied right ventricular papillary muscles. Circ Res 50:491-500, 1982.

Anderson KP: Sudden death, hypertension, and hypertrophy. J Cardiovasc Pharmol 6:S498-S503, 1984.

Anversa P, Loud AV, Giacomelli F, Wiener J: Absolute morphometric study of myocardial hypertrophy in experimental hypertension. II. Ultrastructure of myocytes and interstitium. Lab Invest 38:597-609, 1978.

Anversa P, Loud AV, Vitali-Mazza L: Morphometry and autoradiography of early hypertrophic changes in the ventricular myocardium of adult rat. An electron microscopic study. Lab Invest 35:475-483, 1976.

Anversa P, Ricci R, Olivetti G: Quantitative structural analysis of the myocardium during physiologic growth and induced cardiac hypertrophy: A review. J Am Coll Cardiol 7:1140-1149, 1986.

Aronson RS, Nordin C: Electrophysiologic properties of hypertrophied myocytes isolated from rats with renal hypertension. Europ Heart Journal 5(suppl F):339-345, 1984.

Aronson RS: Afterpotentials and triggered activity in hypertrophied myocardium from rats with renal hypertension. Circ Res 48:720-727, 1981.

Aronson RS: Characteristics of action potentials of hypertrophied myocardium from rats with renal hypertension. Circ Res 47:443-454, 1980.

Assey ME, Wisenbaugh T, Spann Jr JF, Gillette PC, Carabello BA: Unexpected persistence into adulthood of low wall stress in patients with congenital aortic stenosis: Is there a fundamental difference in the hypertrophic response to a pressure overload present from birth? Circulation 75:973-979, 1987.

Bache RJ, Vrobel TR, Ring WS, Emery RW, Andersen RW: Regional myocardial blood flow during exercise in dogs with chronic left ventricular hypertrophy. Circ Res 48:76-87, 1981.

Bishop SP: Ultrastructure of the Myocardium in Physiologic and Pathologic Hypertrophy in Experimental Animals. IN: *Perspectives in Cardiovascular Research, Volume 7, Myocardial Hypertrophy and Failure.* N.R. Alpert (Ed.). New York: Raven Press, 1983, pp 127-147.

Bloor CM: *Cardiac Pathology.* Philadelphia: JB Lippincott Co., 1978, 430 pp.

Braunwald E, Sonnenblick EH, Ross Jr J: Mechanisms of Cardiac Contraction and Relaxation. Chapter 13. IN: *Heart Disease. A Textbook of Cardiovascular Medicine*. E. Braunwald (Ed.). Philadelphia: W.B. Saunders Co., 1988, pp 383-425.

Breisch EA, Houser SR, Carey RA, Spann JF, Bove AA: Myocardial blood flow and capillary density in chronic pressure overload of the feline left ventricle. Cardiovasc Res 14:469-475, 1980.

Brush Jr JE, Cannon III RO, Schenke WH, Bonow RO, Leon MB, Maron BJ, Epstein SE: Angina due to coronary microvascular disease in hypertensive patients without left ventricular hypertrophy. N Engl J Med 319:1302-1307, 1988.

Cameron JS, Myerburg RJ, Wong SS, Gaide MS, Epstein K, Alvarez TR, Gelband H, Guse PA, Bassett AL: Electrophysiologic consequences of chronic experimentally induced left ventricular pressure overload. J Am Coll Cardiol 2:481-487, 1983.

Capasso JM, Aronson RS, Sonnenblick EH: Reversible alterations in excitation-contraction coupling during myocardial hypertrophy in rat papillary muscle. Circ Res 51:189-195, 1982.

Capasso JM, Strobeck JE, Sonnenblick EH: Myocardial mechanical alterations during gradual onset long-term hypertension in rats. Am J Physiol 240:H435-H441, 1981.

Carabello BA, Mee R, Collins Jr JJ, Kloner RA, Levin D, Grossman W: Contractile function in chronic gradually developing subcoronary aortic stenosis. Am J Physiol 240:H80-H86, 1981.

Cranefield PF, Wit AL, Hoffman BF: Genesis of cardiac arrhythmias. Circulation 47:190-204, 1973.

Eichhorn P, Grimm J, Koch R, Hess O, Carroll J, Krayenbuehl HP: Left ventricular relaxation in patients with left ventricular hypertrophy secondary to aortic valve disease. Circulation 65:1395-1403, 1982.

El-Sherif N, Zeiler RH, Craelius W, Gough WB, Henkin R: QTU prolongation and polymorphic ventricular tachyarrhythmias due to bradycardia-dependent early afterdepolarizations. Afterdepolarizations and ventricular arrhythmias. Circ Res 63:286-305, 1988.

Farrer-Brown G: *Color Atlas of Cardiac Pathology*. Chicago: Year Book Medical Publishers, Inc., 1977, 160 pp.

Ferrans VJ: Morphology of the heart in hypertrophy. Cardiac Failure IV. Hosp Prac pp 67-78, 1983.

Fifer MA, Borow KM, Colan SD, Lorell BH: Early diastolic left ventricular function in children and adults with aortic stenosis. J Am Coll Cardiol 5:1147-1154, 1985.

Fozzard HA: Cardiac muscle: Excitability and passive electrical properties. Prog Cardiovasc Dis 19:343-359, 1977.

Friedman M, Manwaring JH, Rosenman RH, Donlon G, Ortega P, Grube SM: Instantaneous and sudden deaths. Clinical and pathological differentiation in coronary artery disease. JAMA 225:1319-1328, 1973.

Frohlich ED: Physiologic considerations in left ventricular hypertrophy. Am J Med 75(2A):12-18, 1983.

Goldstein MA, Sordahl LA, Schwartz A: Ultrastructural analysis of left ventricular hypertrophy in rabbits. J Mol Cell Cardiol 6:265-273, 1974.

Gordon EE, Kira Y, Morgan HE: Aortic perfusion pressure, protein synthesis, and protein degradation. Circulation 75(suppl I):I-78-I-80, 1987.

Gould SE (Ed.): *Pathology of the Heart and Blood Vessels*. Illinois: Charles C. Thomas, 1968, 1198 pp.

Grossman W, Carabello BA, Gunther S, Fifer MA: Ventricular Wall Stress and the Development of Cardiac Hypertrophy and Failure. IN: *Perspectives in Cardiovascular Research, Volume 7, Myocardial Hypertrophy and Failure.* N.R. Alpert (Ed.). New York: Raven Press, 1983, pp 1-18.

Grossman W, Jones D, McLaurin LP: Wall stress and patterns of hypertrophy in the human left ventricle. J Clin Invest 56:56-64, 1975.

Grossman W, McLaurin LP: Diastolic properties of the left ventricle. Annals of Int Med 84:316-326, 1976.

Gwathmey JK, Morgan JP: Altered calcium handling in experimental pressure-overload hypertrophy in the ferret. Circ Res 57:836-843, 1985.

Gülch RW: The effect of elevated chronic loading on the action potential of mammalian myocardium. J Mol Cell Cardiol 12:415-420, 1980.

Hanrath P, Mathey DG, Siegert R, Bleifeld W: Left ventricular relaxation and filling pattern in different forms of left ventricular hypertrophy: An echocardiographic study. Am J Cardiol 45:15-23, 1980.

Henquell L, Odoroff CL, Honig CR: Intercapillary distance and capillary reserve in hypertrophied rat hearts beating in situ. Circ Res 41:400-408, 1977.

Hoffman H, Covell JW: Ventricular and Myocardial Performance in the Hypertrophied Heart. IN: *Perspectives in Cardiovascular Research, Volume 7, Myocardial Hypertrophy and Failure.* N.R. Alpert (Ed.). New York: Raven Press, 1983, pp 261-270.

Hoffman JIE: A critical view of coronary reserve. Circulation 75(suppl I):I-6-I-11, 1987.

Holtz J, Restorff WV, Bard P, Bassenge E: Transmural distribution of myocardial blood flow and of coronary reserve in canine left ventricular hypertrophy. Basic Res Cardiol 72:286-292, 1977.

Huber D, Grimm J, Koch R, Krayenbuehl HP: Determinants of ejection performance in aortic stenosis. Circulation 64:126-134, 1981.

Hutchins GM, Bulkley BH, Moore GW, Piasio MA, Lohr FT: Shape of the human cardiac ventricles. Am J Cardiol 41:646-654, 1978.

Janicki JS, Weber KT, Gochman RF, Shroff S, Geheb FJ: Three-dimensional myocardial and ventricular shape: a surface representation. Am J Physiol 241:H1-11, 1981.

January CT, Riddle JM: Early afterdepolarizations: Mechanism of induction and block. A role for L-Type Ca^{2+} current. Circ Res 64:977-990, 1989.

Jones M, Ferrans VJ: Myocardial Ultrastructure in Children and Adults with Congenital Heart Disease. IN: *Congenital Heart Disease in Adults*. Roberts WC (Ed.). Philadelphia: FA Davis Co., 1980, pp 501-530.

Jouannot P, Hatt PY: Rat myocardial mechanics during pressure-induced hypertrophy development and reversal. Am J Physiol 229:355-364, 1975.

Kannel WB, Doyle JT, McNamara PM, Quickenton P, Gordon T: Precursors of sudden coronary death. Factors related to the incidence of sudden death. Circulation 51:606-613, 1975.

Kannel WB, Gordon T, Offutt D: Left ventricular hypertrophy by electrocardiogram. Prevalence, incidence, and mortality in the Framingham Study. Annals of Int Med 71:89-105, 1969.

Kannel WB: Prevalence and natural history of electrocardiographic left ventricular hypertrophy. Am J Med 75(3A):4-11, 1983.

Kaufmann RL, Homburger H, Wirth H, Disorder in excitation-contraction coupling of cardiac muscle from cats with experimentally produced right ventricular hypertrophy. Circ Res 28:346-357, 1971.

Keung EC: Calcium current is increased in isolated adult myocytes from hypertrophied rat myocardium. Circ Res 64:753-763, 1989.

Keung ECH, Aronson RS: Non-uniform electrophysiological properties and electrotonic interaction in hypertrophied rat myocardium. Circ Res 49:150-158, 1981.

Keung ECH, Keung C-S, Aronson RS: Passive electrical properties of normal and hypertrophied rat myocardium. Am J Physiol 243:H917-H926, 1982.

Lecarpentier Y, Waldenström A, Clergue M, Chemla D, Oliviero P, Martin JL, Swynghedauw B: Major alterations in relaxation during cardiac hypertrophy induced by aortic stenosis in guinea pig. Circ Res 61:107-116, 1987.

Legato MJ: *The Myocardial Cell for the Clinical Cardiologist*. New York: Futura Publishing Co., 1973, 179 pp.

Levine HJ, McIntyre KM, Lipana JG, Bing OHL: Force-velocity relations in failing and nonfailing hearts of subjects with aortic stenosis. Am J Med Sci 259:79-89, 1970.

Lorell BH, Grossman W: Cardiac hypertrophy: The consequences for diastole. J Am Coll Cardiol 9:1189-1193, 1987.

Marcus ML, Doty DB, Hiratzka LF, Wright CB, Eastham CL: Decreased coronary reserve. A mechanism for angina pectoris in patients with aortic stenosis and normal coronary arteries. N Engl J Med 307:1362-1367, 1982.

Marcus ML, Harrison DG, Chilian WM, Koyanagi S, Inou T, Tomanek RJ, Martins JB, Eastham CL, Hiratzka LF: Alterations in the coronary circulation in hypertrophied ventricles. Circulation 75(suppl I), I-19-I-25, 1987.

Marcus ML, Mueller TM, Eastham CL: Effects of short- and long-term left ventricular hypertrophy on coronary circulation. Am J Physiol 241:H358-362, 1981.

Marcus ML, Mueller TM, Gascho JA, Kerber RE: Effects of cardiac hypertrophy secondary to hypertension on the coronary circulation. Am J Cardiol 44:1023-1028, 1979.

Marcus ML: Autoregulation in the Coronary Circulation. Chapter 4. IN: *The Coronary Circulation in Health and Disease.* New York: McGraw-Hill Book Co., 1983a, pp 93-112.

Marcus ML: Metabolic Regulation of Coronary Blood Flow. Chapter 3. IN: *The Coronary Circulation in Health and Disease.* New York: McGraw-Hill Book Co., 1983b, pp 65-92.

Maron BJ, Ferrans VJ: Ultrastructural features of hypertrophied human ventricular myocardium. Prog Cardiovasc Dis 21:207-238, 1978.

Mercadier J-J, Lompré A-M, Wisnewsky C, Samuel J-L, Bercovici J, Swynghedauw B, Schwartz K: Myosin isoenzymic changes in several models of rat cardiac hypertrophy. Circ Res 49:525-532, 1981.

Messerli FH, Ventura HO, Elizardi DJ, Dunn FG, Frohlich ED: Hypertension and sudden death. Increased ventricular ectopic activity in left ventricular hypertrophy. Am J Med 77:18-22, 1984.

Moe GK, Mendez C: Physiologic basis of premature beats and sustained tachycardias. N Engl J Med 288:250-254, 1973.

Morgan HE, Chua BHL, Siehl D, Kira Y, Kochel PJ, Gordon EE: Mechanical factors affecting protein turnover in isolated rat hearts. Federation Proc 45:2563-2567, 1986.

Morgan HE, Gordon EE, Kira Y, Chua BHL, Russo LA, Peterson CJ, McDermott PJ, Watson PA: Biochemical mechanisms of cardiac hypertrophy. Ann Rev Physiol 49:533-543, 1987.

Morgan HE, Gordon EE, Kira Y, Siehl DL, Watson PA, Chua BHL: Biochemical correlates of myocardial hypertrophy. The Physiologist 28:18-27, 1985.

Morkin E: Chronic adaptations in contractile proteins: Genetic regulation. Ann Rev Physiol 49:545-554, 1987.

Mueller TM, Marcus ML, Kerber RE, Young JA, Barnes RW, Abboud FM: Effect of renal hypertension and left ventricular hypertrophy on the coronary circulation in dogs. Circ Res 42:543-549, 1978.

Murray PA, Vatner SF: Reduction of maximal coronary vasodilator capacity in conscious dogs with severe right ventricular hypertrophy. Circ Res 48:25-33, 1981.

O'Keefe DD, Hoffman JIE, Cheitlin R, O'Neill MJ, Allard JR, Shapkin E: Coronary blood flow in experimental canine left ventricular hypertrophy. Circ Res 43:43-51, 1978.

O'Keefe JH, Owen RM, Bove AA: Influence of left ventricular mass on coronary artery cross-sectional area. Am J Cardiol 59:1395-1397, 1987.

Pearlman ES, Weber KT, Janicki JS: Quantitative histology of the hypertrophied human heart. Federation Proc 40:2042-2047, 1981.

Perper JA, Kuller LH, Cooper M: Arteriosclerosis of coronary arteries in sudden, unexpected deaths. 52(suppl III):III-27-III-33, 1975.

Rakusan K, Moravec J, Hatt P-Y: Regional capillary supply in the normal and hypertrophied rat heart. Microvasc Res 20:319-326, 1980.

Rakusan K, Tomanek RJ: Distribution of mitochondria in normal and hypertrophic myocytes from the rat heart. J Mol Cell Cardiol 18:299-305, 1986.

Rappaport L, Swynghedauw B, Mercadier J-J, Lompré A-M, de la Bastie D, Samuel J-L, Schwartz K: Physiological adaptation of the heart to pathological overloading. Federation Proc 45:2573-2579, 1986.

Romo M: Factors related to sudden death in acute ischaemic heart disease. A community study in Helsinki. Acta Medica Scandinavica Supplementum 547:1-92, 1972.

Rosen MR, Wit AL, Hoffman BF: Electrophysiology and pharmacology of cardiac arrhythmias. I. Cellular electrophysiology of the mammalian heart. Am Heart J 88:380-385, 1974.

Sasayama S, Franklin D, Ross Jr J: Hyperfunction with normal inotropic state of the hypertrophied left ventricle. Am J Physiol 232:H418-H425, 1977.

Sasayama S, Ross Jr J, Franklin D, Bloor CM, Bishop S, Dilley RB: Adaptations of the left ventricle to chronic pressure overload. Circ Res 38:172-178, 1976.

Schaper J, Thiedemann K-U, Flameng W, Schaper W: The ultrastructure of sarcomeres in hypertrophied canine myocardium in spontaneous subaortic stenosis. Basic Res Cardiol 69:509-515, 1974.

Schwarz F, Flameng W, Schaper J, Hehrlein F: Correlation between myocardial structure and diastolic properties of the heart in chronic aortic valve disease: Effects of corrective surgery. Am J Cardiol 42:895-903, 1978.

Simon H, Krayenbuehl HP, Rutishauser W, Preter BO: The contractile state of the hypertrophied left ventricular myocardium in aortic stenosis. Am Heart J 79:587-602, 1970.

Spann JF, Bove AA, Natarajan G, Kreulen T: Ventricular performance, pump function and compensatory mechanisms in patients with aortic stenosis. Circulation 62:576-582, 1980.

Spann Jr JF, Buccino RA, Sonnenblick EH, Braunwald E: Contractile state of cardiac muscle obtained from cats with experimentally produced ventricular hypertrophy and heart failure. Circ Res 21:341-354, 1967.

Takahashi M, Sasayama S, Kawai C, Kotoura H: Contractile performance of the hypertrophied ventricle in patients with systemic hypertension. Circulation 62:116-126, 1980.

Tomanek RJ, Palmer PJ, Peiffer GL, Schreiber KL, Eastham CL, Marcus ML: Morphometry of canine coronary arteries, arterioles, and capillaries during hypertension and left ventricular hypertrophy. Circ Res 58:38-46, 1986.

Toyoshima H, Yung-Dae P, Ishikawa Y, Nagata S, Hirata Y, Sakakibara H, Shimomura K, Nakayama R: Effect of ventricular hypertrophy on conduction velocity of activation front in the ventricular myocardium. Am J Cardiol 49:1938-1945, 1982.

Tritthart H, Luedcke H, Bayer R, Stierle H, Kaufmann R: Right ventricular hypertrophy in the cat - An electrophysiological and anatomical study. J Mol Cell Cardiol 7:163-174, 1975.

Vrobel TR, Ring WS, Anderson RW, Emery RW, Bache RJ: Effect of heart rate on myocardial blood flow in dogs with left ventricular hypertrophy. Am J Physiol 239:H621-H627, 1980.

Walsh R, Freeman G, Cragg D, Crawford M, Shade R: Load independent impaired ventricular relaxation in hypertrophied baboons. (Abstract) Circulation 72(suppl III):III-485, 1985.

Weber KT, Janicki JS, Pick R, Abrahams C, Shroff SG, Bashey RI, Chen RM: Collagen in the hypertrophied, pressure-overloaded myocardium. Circulation 75(suppl I):I-40-I-47, 1987.

Weber KT, Janicki JS, Shroff SG, Pick R, Chen RM, Bashey RI: Collagen remodeling of the pressure-overloaded, hypertrophied nonhuman primate myocardium. Circ Res 62:757-765, 1988.

Wexler LF, Lorell BH, Momomura S, Weinberg EO, Ingwall JS, Apstein CS: Enhanced sensitivity to hypoxia-induced diastolic dysfunction in pressure-overload left ventricular hypertrophy in the rat: Role of high-energy phosphate depletion. Circ Res 62:766-775, 1988.

White CW, Mirro MJ, Lund DD, Skorton DJ, Pandian NG, Kerber RE: Alterations in ventricular excitability in conscious dogs during development of chronic heart failure. Am J Physiol 250:H1022-H1029, 1986.

Yin FCP, Spurgeon HA, Weisfeldt ML, Lakatta EG: Mechanical properties of myocardium from hypertrophied rat hearts. A comparison between hypertrophy induced by senescence and by aortic banding. Circ Res 46:292-300, 1980.

Yin FCP: Ventricular wall stress. Circ Res 49:829-842, 1981.

Zipes DP: Genesis of Cardiac Arrhythmias: Electrophysiological Considerations. Chapter 20. IN: *Heart Disease. A Textbook of Cardiovascular Medicine.* E. Braunwald (Ed.). Philadelphia: W.B. Saunders Co., 1988, pp 581-620.